BIOCHEMISTRY
including biophysical chemistry & molecular biology

Article

pubs.acs.org/biochemistry

Importance of the C2, N7, and C8 Positions to the Mutagenic Potential of 8-Oxo-2′-deoxyguanosine with Two A Family Polymerases

Michelle L. Hamm,* Kelly A. Crowley, Michael Ghio, Laura Del Giorno, Margaret A. Gustafson, Kevin E. Kindler, Claire W. Ligon, Maria A. M. Lindell, Emily J. McFadden, Carlos Siekavizza-Robles, and Matthew R. Summers

Department of Chemistry, University of Richmond, Gottwald B-100, Richmond, Virginia 23173, United States

Supporting Information

ABSTRACT: 8-Oxo-2′-deoxyguanosine (OdG) is a prominent DNA lesion produced from the reaction of 2′-deoxyguanosine (dG) with reactive oxygen species. While dG directs the insertion of only dCTP during replication, OdG can direct the insertion of either dCTP or dATP, allowing for the production of dG → dT transversions. When replicated by Klenow fragment-exo (KF-exo), OdG preferentially directs the incorporation of dCTP over dATP, thus decreasing its mutagenic potential. However, when replicated by a highly related polymerase, the large fragment of polymerase I from *Bacillus stearothermophilus* (BF), dATP incorporation is preferred, and a higher mutagenic potential results. To gain insight into the reasons for this opposite preference and the effects of the C2, N7, and C8 positions on OdG mutagenicity, single-nucleotide insertions of dCTP and/or dATP opposite dG, OdG, and seven of their analogues were examined by steady state kinetics with both KF-exo and BF. Results from these studies suggest that the two enzymes behave similarly and are both sensitive not only to steric and electronic changes within the imidazole ring during both dCTP and dATP incorporation but also to the presence of the C2-exocyclic amine during dATP incorporation. The difference in incorporation preference opposite OdG appears to be due to a somewhat increased sensitivity to structural perturbations during dCTP incorporation with BF. Single-nucleotide extensions past the resulting base pairs were also studied and were not only similar between the two enzymes but also consistent with published ternary crystallographic studies with BF. These results are analyzed in the context of previous biochemical and structural studies, as well as stability studies with the resulting base pairs.

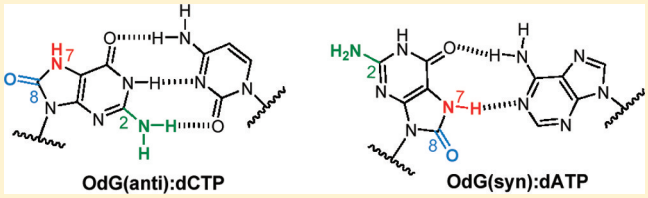

8-Oxo-2′-deoxyguanosine [OdG (Chart 1)] is a common DNA lesion that arises from the exposure of 2′-deoxyguanosine (dG) to reactive oxygen species (ROS) that include hydroxy radical ($^{\bullet}OH$), peroxides (H_2O_2), and superoxide ($O_2^{\bullet-}$).[1,2] ROS are produced by environmental carcinogens, during exposure to radiation, and during the conversion of O_2 to H_2O in metabolic respiration.[3−8] While OdG lesions do not serve as either replication or transcription blocks, they are a known promutagen. In vivo studies have shown that OdG has a 0.7−4% mutation rate, with the vast majority being dG → dT transversions.[9,10] It is believed that these mutations may be responsible for the known link between OdG lesions and aging,[11−13] as well as numerous diseases, including cancer.[14−17]

OdG can exist in different tautomeric states, but the 6,8-diketo form predominates at physiological pH.[18,19] In this state, the hydrogen bonding pattern of the imidazole ring is considerably different from that in dG. In OdG the hydrogen at N7 can act as a hydrogen bond donor and the oxygen at C8 can accept a hydrogen bond, while in dG, the N7 can only accept hydrogen bonds and there is no hydrogen bonding ability at C8. Additionally, the presence of the oxygen at C8 imparts additional steric bulk off the imidazole ring, which causes OdG to prefer a syn conformation about the glycosidic bond, as compared to dG, which prefers an anti conformation.[18,19] Together, these changes in base conformation and hydrogen bonding are believed to be responsible for the ability of OdG to form stable base pairs to both 2′-deoxycytidine (dC) and 2′-deoxyadenosine [dA (Chart 2)].[20] When in the syn conformation, OdG can use its Hoogsteen edge to form a relatively stable base pair with dA that structurally mimics an unmodified dT:dA base pair.[21,22] However, OdG can also adopt the anti conformation and form a more standard base pair with dC,[23,24] though OdG:dC base pairs are less stable than dG:dC base pairs.[20]

Because OdG:dC and OdG:dA base pairs both mimic natural base pairs and have similar stabilities, polymerases can have trouble distinguishing between them. Consequently, a polymerase may pair a template OdG lesion with either dCTP or dATP during replication.[21] While insertion of dCTP should cause no harm to the cell, if a dATP is inserted, subsequent rounds of

Received: September 1, 2011
Revised: October 31, 2011
Published: November 14, 2011

Chart 1. Structures and Abbreviations of Nucleotides Used in This Study

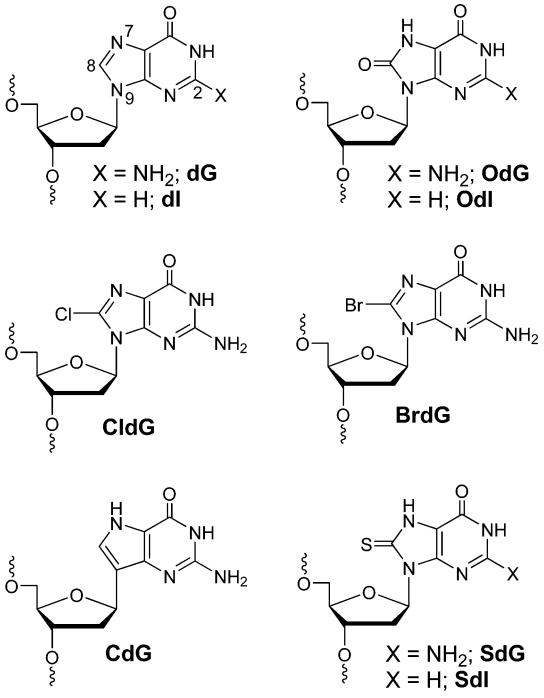

Chart 2. Structures of OdG:dC and OdG:dA Base Pairs

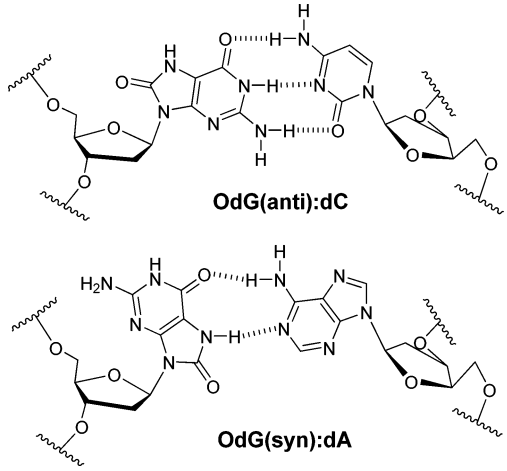

replication will yield the aforementioned dG → dT transversion. Thus, the potential for OdG to cause a mutation is heavily influenced by the polymerase used to replicate it. If a polymerase preferentially pairs OdG with dCTP, the mutagenic potential of OdG would be limited. However, if a polymerase prefers an OdG:dATP pairing, an increased mutagenic potential would result. Polymerases are known to have widely varying incorporation preferences opposite OdG, with some strongly preferring dCTP incorporation,[25−28] several having only a slight preference for dCTP,[29−31] and others strongly preferring dATP incorporation.[21,32,33] Though it may be expected that DNA polymerases from different families would have very different incorporation preferences opposite OdG, it is somewhat surprising that contrary preferences are found even within the same family. For example, the A family polymerase Klenow fragment from *Escherichia coli* DNA polymerase I (KF) that lacks the 3′-exonuclease site (KF-exo) prefers to insert dCTP ∼4-fold over dATP opposite OdG,[30] while a highly related A family polymerase, the large fragment from *Bacillus stearothermophilus* (BF), prefers dATP incorporation by ∼9-fold.[34] In the B family of DNA polymerases, human pol α prefers dATP insertion by ∼200-fold,[21] while the replicative DNA polymerase from bacteriophage RB69 (RB69) prefers dCTP incorporation by ∼20-fold.[26] Other examples exist, as well.[27,32]

To gain insight into the reasons for these opposite incorporation preferences within the same polymerase family, we set about testing the activity of dCTP and dATP incorporation opposite numerous dG/OdG analogues with both KF-exo and BF. These two A family polymerases were chosen because they show strong structural and sequence homology,[35,36] replication past OdG and its analogues has been extensively studied with KF-exo,[30,37−41] and there are numerous crystal structures of BF available.[34,42,43] The analogues examined vary from dG/OdG at N7 and C8 (the two sites that differ between dG and OdG), as well as at C2, and include (i) 8-chloro-2′-deoxyguanosine [CldG (Chart 1)] and 8-bromo-2′-deoxyguanosine (BrdG), which contain steric bulk at C8 similar to that of OdG but otherwise mimic dG, (ii) 9-deaza-2′-deoxyguanosine (CdG) and 8-thio-2′-deoxyguanosine (SdG), which contain the N7-hydrogen used when pairing to dA but differ from OdG in their steric and electronic properties at C8, and (iii) 2′-deoxyinosine (dI), 8-oxo-2′-deoxyinosine (OdI), and 8-thio-2′-deoxyinosine (SdI), which all lack an C2-exocyclic amine but otherwise mimic dG, OdG, and SdG, respectively. Studies of the incorporation opposite and extension past these analogues in comparison to OdG with both KF-exo and BF should yield more information about not only how the various steric and electronic properties of C2, N7, and C8 influence the mutagenic potential of OdG but also why highly related polymerases can have widely differing incorporation preferences opposite OdG. Only by understanding the specific properties and interactions that dictate the mutagenic potential of OdG can we fully understand its potential to cause mutation and disease.

EXPERIMENTAL PROCEDURES

All chemicals were purchased from Sigma-Aldrich unless otherwise noted. KF-exo (20000 units/mg) and BF (120000 units/mg) were purchased from NEB. Oligonucleotide synthesis was conducted at the Biomolecular Research Facility at the University of Virginia (CldG, CdG, and SdG) or by Midland Inc. (OdI and SdI). Matrix-assisted laser desorption ionization time-of-flight mass spectrometry analysis was conducted at the Mass Spectrometry Facility at the University of California (Riverside, CA). Preparative reverse phase high-performance liquid chromatography (RP-HPLC) was performed using a Beckman Ultrasphere ODS C18 column (10 mm × 250 mm) run at 3 mL/min; HPLC solvents A and B were 0.1 M triethylammonium acetate (TEAAC) (pH 7) and acetonitrile, respectively.

8-[2-(Trimethylsilyl)ethyl]thio-2′-deoxyinosine (2). 8-Bromo-2′-deoxyinosine (**1**, 300 mg, 0.90 mmol)[44] and 600 mg of K_2CO_3 (4.3 mmol) were suspended in 4 mL of dry *N*,*N*-dimethylformamide (DMF) before the addition of 420 μL (2.7 mmol) of 2-(trimethylsilyl)ethanethiol. The mixture was stirred under argon at 60 °C for 20 h before being concentrated in vacuo. The resulting residue was washed twice with hexane, dried, and dissolved into methanol. The solid was filtered, and the filtrate was dried to yield 420 mg of impure **2** as a yellow

dx.doi.org/10.1021/bi201383c | *Biochemistry* 2011, 50, 10713−10723

solid. Though the impure product was used in the subsequent step to make compound **3**, compound **2** could be purified by reverse phase C_{18} column chromatography using a 0 to 40% CH_3CN gradient in water to yield 130 mg (0.34 mmol, 38% yield) of pure **2** as a white solid: ^{1}H NMR (300 MHz, DMSO-d_6) δ 7.99 (s, 1H), 6.21 (t, 1H), 5.31 (b, 1H), 4.95 (b, 1H), 4.41 (m, 1H), 3.84 (m, 1H), 3.63 (dd, 1H), 3.50 (dd, 1H), 3.28 (m, 2H), 3.03 (m, 1H), 2.14 (ddd, 1H), 1.01 (m, 2H), 0.061 (s, 8H); ^{13}C NMR (300 MHz, DMSO-d_6) δ 156.4, 149.9, 147.7, 145.6, 125.5, 88.5, 84.8, 71.5, 62.5, 40.9, 40.6, 40.3, 40.0, 39.8, 39.5, 39.2, 37.8, 29.2, 17.2, −1.2; HR-ESI (MH^+) for $C_{15}H_{25}N_4O_4SiS$ expected 385.1360, found 385.1365.

5′-*O*-Dimethoxytrityl-8-[2-(trimethylsilyl)ethyl]thio-2′-deoxyinosine (3). Impure **2** (436 mg) was coevaporated three times with pyridine to remove any associated water before addition of 1.35 g (3.97 mmol) of dimethoxytrityl chloride and 7 mg (0.057 mmol) of 2-(dimethylamino)pyridine. The mixture was covered with argon, and 8 mL of anhydrous pyridine and 316 μL (2.27 mmol) of triethylamine were added. After being stirred at 35 °C for 8 h, the mixture was concentrated, and the resulting oil was purified by silica gel chromatography using a 0 to 4% methanol gradient in chloroform to yield 239 mg of compound **3** (0.327 mmol, 36% yield over two steps from compound **1**) as an orange foam: ^{1}H NMR (500 MHz, $CDCl_3$-d_6) δ 7.76 (s, 1H), 7.43 (d, 2H), 7.41−7.24 (m, 7H), 6.78 (dd, 4H), 6.36 (t, 1H), 4.84 (m, 1H), 4.11 (m, 1H), 3.78 (s, 3H), 3.77 (s, 1H), 1.50 (dd, 1H), 3.44 (m, 2H), 3.38 (dd, 1H), 3.30 (m, 1H), 2.34 (ddd, 1H), 1.01 (m, 2H), 0.089 (s, 8H); ^{13}C NMR (500 MHz, $CDCl_3$-d_6) δ 158.5, 158.5, 158.3, 150.8, 150.3, 149.8, 144.7, 142.7, 136.1, 136.0, 135.9, 130.1, 130.0, 128.2, 127.8, 126.9, 125.3, 123.8, 113.1, 86.4, 85.7, 84.3, 73.1, 64.0, 55.2, 37.5, 29.3, 16.6, −1.7; HR-ESI (MNa^+) for $C_{36}H_{42}N_4O_6NaSiS$ expected 709.2487, found 709.2495.

5′-*O*-Dimethoxytrityl-8-[2-(trimethylsilyl)ethyl]thio-2′-deoxyinosine-3′-yl-β-cyanoethyl-*N*,*N*-diisopropyl-phosphoramidite (4). Compound **3** (184 mg, 0.26 mmol) was coevaporated three times with pyridine to remove any associated water before the addition of 41 mg (0.35 mmol) of dicyanoimidazole. The flask was covered with argon, and 5 mL of anhydrous methylene chloride and 100 μL (0.31 mmol) of 2-cyanoethyl *N*,*N*,*N*′,*N*′-tetraisopropylphosphorodiamidite (Chemgenes) were added. The mixture was stirred for 30 min at room temperature, diluted with 10 mL ethyl acetate, and washed twice with 10 mL of a saturating sodium bicarbonate solution. The organic layer was dried with Na_2SO_4 and concentrated in vacuo. The resulting solid was purified by silica gel chromatography using a 6 to 20% acetone gradient and 0.1% triethylamine in methylene chloride that had been run through alumina to yield 162 mg of compound **4** (0.18 mmol, 70% yield) as a white foam: ^{31}P NMR ($CDCl_3$) δ 148.9, 148.5; HR-MS (MNa^+) for $C_{45}H_{59}N_6O_7NaSiPS$ expected 909.3565, found 909.3580.

Oligonucleotide Synthesis. For the polymerase experiments, template oligonucleotides were 5′-d(TCACXCTGCTGTCGG)-3′, where X is dG, BrdG, CldG, CdG, OdG, SdG, dI, OdI, or SdI, while primer oligonucleotides used for the incorporation experiments were 5′-d(CCGACAGCAG)-3′; primers used for the extension experiments were 5′-d(CCGACAGCAGY)-3′, where Y is either dC or dA. Oligonucleotides used in the melting studies were 5′-d(CCATCXCTACC)-3′, where X is dG, BrdG, CldG, CdG, OdG, SdG, dI, OdI, or SdI, while the complements used were 5′-d(GGTAGYGATGG)-3′, where Y is dC or dA. Unmodified oligonucleotides were purchased from IDT DNA, while oligonucleotides containing dI, OdG, and BrdG were purchased from Midland Inc. Oligonucleotides containing SdG,[45] CldG,[46] CdG,[47] and OdI[39] were synthesized as previously described. The phosphoramidite derivative of OdI was a generous gift from M. Greenberg.

Oligonucleotide Purification. All oligonucleotides were purified by 20% denaturing polyacrylamide gel electrophoresis (PAGE) before ultraviolet (UV) visualization. The slowest running band was excised and soaked twice in water, in the dark, for 24 h. The resulting solutions were then concentrated, combined by resuspension in 1 mL of water, and filtered. The oligonucleotides (except those containing SdG and SdI) were then further purified by preparative RP-HPLC using a linear gradient from 5 to 20% B in A over 30 min.

Oligonucleotides containing the protected SdG and SdI derivatives were gel purified as described above before further purification by preparative RP-HPLC using a linear gradient from 5 to 60% B in A over 30 min. The collected fractions were dried in vacuo before addition of 0.3 mL of 1.0 M TBAF in THF to deprotect the sulfur. The solution was mixed well, covered with argon, and wrapped in foil. After 30 min at room temperature, the reaction was quenched with 0.3 mL of 1.0 M TEAAC, and the THF was removed by concentration. The samples were then purified with a NAP-5 column (Amersham).

Melting Studies. A solution with each oligonucleotide at 2 μM, 100 mM NaCl, 10 mM $MgCl_2$, and 10 mM PIPES buffer (pH 7) was heated for 5 min at 90 °C before being slowly cooled to room temperature for at least 30 min and then to 20 °C for at least 10 min. Melting temperatures were determined on a Cary 100 UV−vis spectrophotometer with a Peltier temperature controller. The absorbance at 260 nm was monitored from 20 to 80 °C with the temperature increased at a rate of 0.5 °C/min. Melting temperatures (T_m) were determined by a computer fit of the first derivative of absorbance with respect to $1/T$.

Radiolabeling of Primers. Primers were radiolabeled using Optikinase (USB) and [γ-^{32}P]ATP (MP Biomedical) and purified using mini Quick Spin Oligo Columns (Roche).

Insertion and Extension Experiments with KF-exo. Solutions containing Tris-HCl, $MgCl_2$, EDTA, β-mercaptoethanol, BSA, template, and primer were heated at 90 °C for 3 min before being slowly cooled to room temperature. KF-exo was then added so that the final concentrations in the solution were 50 mM Tris-HCl (pH 7.5), 20 mM $MgCl_2$, 2 mM EDTA, 1.6 mM β-mercaptoethanol, 5 μg/mL BSA, 0.1 μM template, 0.1 μM ^{32}P-radiolabeled primer (10mer for insertion or 11mer for extension), and 0.37 nM KF-exo in 10% glycerol (except for incorporation of dCTP opposite SdI and extension past SdG:dC and SdI:dC base pairs, which each contained 3.7 nM KF-exo). Five microliters of the solution described above was incubated at 25 °C for 5 min and then added to 5 μL of a 2× dNTP solution (that had also been incubated at 25 °C for 5 min) containing 100 mM Tris-HCl (pH 7.5), 20 mM $MgCl_2$, and the appropriate dNTP concentration. After the appropriate time, reactions were stopped with 20 μL of a solution containing 95% formamide, 20 mM EDTA, 0.0025% bromophenol blue, and 0.0025% xylene cyanol.

It should be noted that some commercially purchased KF-exo has contaminating pyrophosphate that can induce pyrophosphorolysis.[39,41] We saw little evidence of this in control studies under our conditions. Additionally, qualitative

controls in our lab showed that experiments with KF-exo that had been pretreated with pyrophosphatase gave results similar to those obtained with untreated KF-exo.

Insertion and Extension Experiments with BF. Solutions containing Tris-HCl, $MgCl_2$, DTT, BSA, template, and primer were heated at 90 °C for 3 min before being slowly cooled to room temperature. BF was then added so that the final concentrations in the solution were 100 mM Tris-HCl (pH 8), 10 mM $MgCl_2$, 2 mM DTT, 5 μg/mL BSA, 0.2 μM template, 0.4 μM ^{32}P-radiolabeled primer (10mer for insertion or 11mer for extension), and 1.3 or 0.25 nM BF in 10% glycerol for insertion or extension, respectively (13 nM BF was used during incorporation of dATP and dCTP opposite dI and SdG, respectively, 33 nM BF for incorporation of dCTP opposite SdI, and 2.5 nM BF for extension past SdI:dC base pairs). Five microliters of the solution described above was incubated at 25 °C for 5 min and then added to 5 μL of a 2× dNTP solution (that had also been incubated at 25 °C for 5 min) containing 20 mM NaCl and the appropriate dNTP concentration. After the appropriate time, reactions were stopped with 20 μL of a solution containing 95% formamide, 20 mM EDTA, 0.0025% bromophenol blue, and 0.0025% xylene cyanol before the mixtures were heated at 90 °C for 5 min.

Separation of Product and Michealis–Menten Kinetics. Product oligonucleotides were separated from starting oligonucleotides using 20% denaturing PAGE. The resulting gel was dried, exposed to a storage phorphor screen (Amersham) overnight, and visualized using a Storm 860 Phosphorimager (Amersham). Steady state kinetic experiments were conducted under initial conditions where ≤20% of the reaction had progressed and included seven different dNTP concentrations. Reagent and product bands were quantified using ImageQuant version 5.0. Michaelis–Menten curves were generated using values obtained from the averaging of at least three replicates and were repeated at least three times to ensure accuracy. k_{cat} and K_m values were obtained directly from the Michaelis–Menten curves using SigmaPlot version 9.0.

RESULTS

Synthesis of SdI Phosphoramidite. The phosphoramidite derivative of SdI (compound **4**), which is required for solid phase DNA synthesis, has not been previously reported. To generate this compound, we used chemistry similar to that previously developed for the synthesis of SdG.[45] After 8-bromo-2′-deoxyinosine (compound **1**)[44] was prepared from 8-bromo-2′-deoxyadenosine,[48] essentially as previously reported, it was reacted with 2-(trimethylsilyl)ethanethiol to yield the protected SdI derivative **2** (Scheme 1). While this compound could be purified through reverse phase chromatography, crude material was used in the subsequent step where the 5′-hydroxyl was protected as a dimethoxytrityl (DMTr) ether. The 3′-hydroxyl was then activated as a phosphoramidite through standard chemistry to yield the solid phase synthesis ready SdI derivative **4**. The phosphoramidite coupled with 95% efficiency under standard conditions.

Oligonucleotide Synthesis. Oligonucleotides containing dG, BrdG, OdG, and dI are commercially available, while oligonucleotide incorporation of CldG, CdG, SdG, and OdI and their subsequent purification have been previously reported.[39,45−47] Oligonucleotides containing the protected SdI derivative were synthesized, purified, and deprotected according to procedures developed for oligonucleotides containing SdG.[45]

Scheme 1. Synthesis of the Phosphoramidite Derivative of SdI

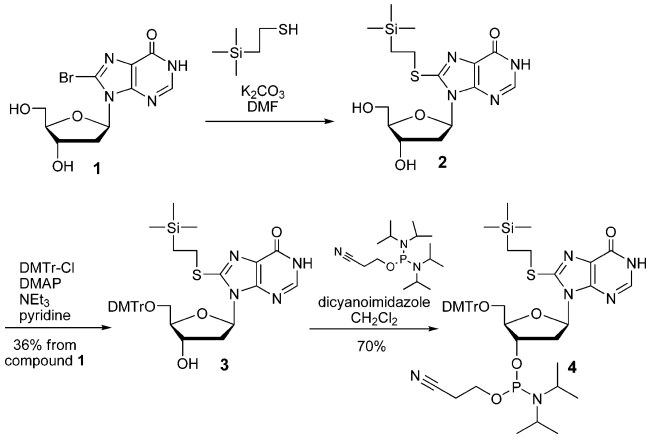

Base Pair Thermal Stabilities. UV melting studies of 11-nucleotide duplexes were used to compare the thermal base pair stability of the OdG analogues opposite dC or dA. Because all duplexes were melted under the same conditions and contained the same sequence except at the one base pair, the stabilities of the varying base pairs can be compared directly. The results in Table 1 are similar to those previously reported

Table 1. Melting Temperatures (T_m, °C) of DNA Duplexes[a]

5′-CCATCXCTACC-3′
3′-GGTAGYGATGG-5′

X	Y = dC	Y = dA
dG	54.8 ± 0.5	40.1 ± 0.4
CldG	49.1 ± 0.1	35.0 ± 0.4
BrdG	47.0 ± 0.4	36.6 ± 0.4
CdG	51.4 ± 0.5	43.5 ± 0.4
OdG	50.3 ± 0.4	44.9 ± 0.2
SdG	43.7 ± 0.3	44.6 ± 0.4
dI	48.0 ± 0.6	44.6 ± 0.3
OdI	43.5 ± 0.5	45.8 ± 0.5
SdI	36.8 ± 0.3	45.2 ± 0.3

[a]Conditions: 2 μM duplex, 10 mM PIPES (pH 7), 100 mM NaCl, and 10 mM $MgCl_2$. Average T_m values ± the standard deviations were calculated from three or more melts.

and further confirm that (i) the removal of the C2-exocyclic amine and the presence of a large atom off C8 of dG each destabilize base pairs with dC,[39,46,49] (ii) OdG:dC (and SdG:dC) base pairs show destabilization beyond what is expected solely on the basis of the atomic size off C8,[46] possibly because of electronic differences within the imidazole ring,[50] (iii) the increased atomic size off C8 of OdG has little to no effect on the stability of OdG:dA base pairs,[45] and (iv) removal of the C2-exocyclic amine may have a small stabilizing effect on OdG:dA base pairs.[39] Additionally, it is well-known that dI can form relatively stable base pairs with dA where the dI is in an anti conformation, and the dA can adopt either a syn or anti conformation.[51,52] Though one can imagine OdI and SdI adopting similar pairings with dA, these structures would be highly unlikely because of the oxygen or sulfur at C8, which would significantly destabilize the required anti conformation.[46,53] Because OdI:dA and SdI:dA base pairs are more thermally stable than a dI:dA pair, as well as OdI:dC and SdI:dC pairs, it is much more likely that both OdI and SdI

Table 2. Kinetic Parameters for Steady State Incorporation of dCTP or dATP with KF-exo and BF

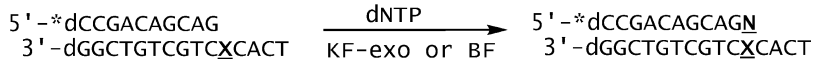

	KF-exo				BF			
X:dNTP	k_{cat} (min^{-1})[a]	K_m(dNTP) (μM)[a]	k_{cat}/K_m (min^{-1} μM^{-1})	dCTP/dATP[b]	k_{cat} (min^{-1})[a]	K_m(dNTP) (μM)[a]	k_{cat}/K_m (min^{-1} μM^{-1})	dCTP/dATP[b]
dG:dCTP	200 ± 40	0.22 ± 0.08	910 ± 380		330 ± 100	1.5 ± 0.5	220 ± 100	
ClдG:dCTP	290 ± 70	7.3 ± 1.8	40 ± 13		280 ± 74	81 ± 28	3.4 ± 1.5	
BrdG:dCTP	330 ± 100	13 ± 7	25 ± 16		94 ± 20	130 ± 70	0.72 ± 0.40	
CdG:dCTP	130 ± 30	4.2 ± 1.6	31 ± 14	0.33	600 ± 210	45 ± 7	13 ± 5	15
CdG:dATP	67 ± 20	0.72 ± 0.06	93 ± 28		58 ± 3	66 ± 23	0.89 ± 0.31	
OdG:dCTP	160 ± 40	16 ± 5	10 ± 4	6.7	12 ± 3	150 ± 10	0.080 ± 0.021	0.22
OdG:dATP	19 ± 3	13 ± 1	1.5 ± 0.2		24 ± 4	66 ± 20	0.36 ± 0.15	
SdG:dCTP	23 ± 3	13 ± 4	1.8 ± 0.6	13	0.42 ± 0.10	65 ± 14	0.0065 ± 0.0020	0.50
SdG:dATP	1.9 ± 0.2	14 ± 2	0.14 ± 0.02		3.5 ± 0.6	270 ± 120	0.013 ± 0.006	
dI:dCTP	70 ± 25	0.22 ± 0.07	320 ± 150	820	18 ± 4	0.12 ± 0.04	150 ± 60	30000
dI:dATP	7.8 ± 1.4	20 ± 3	0.39 ± 0.09		1.3 ± 0.03	260 ± 80	0.0050 ± 0.0018	
OdI:dCTP	94 ± 16	50 ± 16	1.9 ± 0.7	0.23	52 ± 10	380 ± 50	0.14 ± 0.03	0.067
OdI:dATP	97 ± 20	12 ± 4	8.1 ± 3.1		140 ± 45	66 ± 13	2.1 ± 0.8	
SdI:dCTP	4.4 ± 0.8	86 ± 13	0.051 ± 0.012	0.10	0.25 ± 0.05	30 ± 7	0.0083 ± 0.0024	0.16
SdI:dATP	8.3 ± 1.9	17 ± 3	0.49 ± 0.14		3.9 ± 0.1	77 ± 12	0.051 ± 0.008	

[a]Averages ± standard deviations calculated from three or more experiments. [b]dCTP/dATP = $(k_{cat}/K_m)_{dCTP}/(k_{cat}/K_m)_{dATP}$.

mimic OdG when pairing to dA and adopt a syn conformation (Chart 2).

Insertion of dCTP and dATP opposite dG, OdG, or Their Analogues. Single-nucleotide insertion experiments were performed using steady state kinetics. Oligonucleotide templates (15 nucleotides long) that contained dG, OdG, or one of the seven analogues were paired with a 5′-radiolabled 10-nucleotide primer and tested for activity with KF-exo or BF (Table 2), which both lack a competing exonuclease function. Though it is possible minor tautomers of OdG can direct incorporation of other dNTPs besides dCTP and dATP,[54,55] little evidence of this was detected in control experiments with dG, OdG, or the analogues. There was some incorporation of dTTP opposite dG and dI observed with higher enzyme concentrations; however, very little of this mismatch was produced opposite OdG or any of the other analogues (see Figures S1 and S2 of the Supporting Information); thus, the kinetic parameters for dGTP or dTTP incorporation were not determined. The reaction parameters for incorporation of dATP opposite dG, ClдG, and BrdG were also not quantified because these experiments were too slow to accurately measure (see Figures S1 and S2 of the Supporting Information). Additionally, dG, ClдG, and BrdG all lack a hydrogen at N7; thus, their kinetic parameters would not provide much insight into the insertion of dATP opposite OdG.

Our results with OdG with both polymerases are comparable to previous findings. In this study, KF-exo had an almost 7-fold preference for insertion of dCTP opposite OdG (Table 2), similar to the 7- and 4-fold dCTP preferences published for KF[21] and KF-exo,[30] respectively. BF was previously shown to prefer dATP incorporation 9-fold over dCTP incorporation,[34] compared to the almost 5-fold preference for dATP reported here. Additionally, the reduction in efficiency observed when dCTP is inserted opposite OdG as compared to dG also mirrored past data. Previous studies found 280- and 3800-fold reductions in efficiency for KF-exo and BF, respectively,[30,34] whereas herein, reaction efficiencies were reduced 91- and 2800-fold, respectively.

Upon examination of the new work with the analogues (Table 2), similar results and trends were observed with both enzymes; dCTP incorporations were less efficient opposite all seven analogues than opposite dG, with incorporations opposite SdG and SdI the least efficient overall. Upon comparison of the individual reaction parameters, it was found that with KF-exo, the rate of dCTP incorporation was actually faster opposite ClдG and BrdG as compared to dG, but the level of dCTP binding was much reduced, yielding 23- and 36-fold less efficient reactions, respectively. Conversely, with BF, both a slower rate and decreased dCTP binding affinity lead to the overall 65- and 310-fold decreases in dCTP insertion efficiency observed for ClдG and BrdG, respectively. OdG and SdG also directed less efficient incorporation of dCTP as compared to dG with both polymerases, though both the rates and dCTP binding affinities were reduced in all cases, leading to reactions that were even less efficient than those opposite ClдG and BrdG. Although it does not significantly differ in size from dG, the C nucleotide analogue CdG directed dCTP insertion less efficiently than dG with both enzymes, though the reaction was more efficient than opposite OdG or SdG. While removal of the C2-exocyclic amine reduced the efficiency of incorporation of dCTP with KF-exo (incorporations opposite OdI and SdI were less efficient than those opposite OdG and SdG, respectively), the same perturbation slightly increased the efficiency with BF.

With regard to dATP incorporation, with KF-exo, the efficiency was highest opposite CdG, because of both a faster rate and tighter binding of dATP, with large decreases in efficiency of 62- and 660-fold when dATP was inserted opposite OdG and SdG, respectively (Table 2). With BF, there was also a reduction in the efficiency of incorporation of dATP through the series CdG, OdG, and SdG, with reactions opposite SdG having both the slowest rate and highest K_m. Removal of the C2-exocyclic amine yielded similar effects with both polymerases; the efficiencies of insertion of dATP opposite OdI and SdI were all increased between 4- and 6-fold as compared to opposite OdG and SdG, respectively.

dx.doi.org/10.1021/bi201383c | Biochemistry 2011, 50, 10713–10723

Table 3. Kinetic Parameters for Steady State Extension past Base Pairs to dC and dA with KF-exo and BF

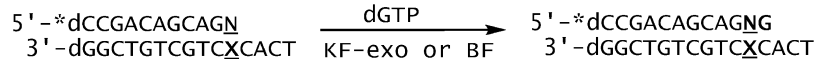

	KF-exo			BF		
X:N	k_{cat} (min^{-1})[a]	K_m(dNTP) (μM)[a]	k_{cat}/K_m (min^{-1} μM^{-1})	k_{cat} (min^{-1})[a]	K_m(dNTP) (μM)[a]	k_{cat}/K_m (min^{-1} μM^{-1})
dG:dC	310 ± 20	0.27 ± 0.04	1100 ± 200	1500 ± 200	7.2 ± 1.2	210 ± 40
CldG:dC	89 ± 11	3.5 ± 0.9	25 ± 7	540 ± 110	9.1 ± 3.0	59 ± 23
BrdG:dC	33 ± 6	3.5 ± 1.0	9.4 ± 3.1	430 ± 10	9.5 ± 2.6	45 ± 12
CdG:dC	130 ± 6	2.7 ± 0.2	48 ± 4	800 ± 120	12 ± 3	67 ± 19
CdG:dA	15 ± 3	3.5 ± 1.5	4.3 ± 1.5	360 ± 60	26 ± 6	14 ± 4
OdG:dC	4.4 ± 0.3	2.3 ± 0.5	1.9 ± 0.4	77 ± 22	24 ± 4	3.2 ± 1.2
OdG:dA	110 ± 30	2.2 ± 0.5	50 ± 17	1100 ± 270	10 ± 3	110 ± 43
SdG:dC	0.47 ± 0.06	1.2 ± 0.03	0.39 ± 0.11	32 ± 3	12 ± 4	2.7 ± 0.9
SdG:dA	58 ± 11	2.1 ± 0.2	28 ± 6	870 ± 200	12 ± 3	73 ± 25
dI:dC	670 ± 90	0.10 ± 0.03	6700 ± 2200	770 ± 280	72 ± 26	11 ± 5
OdI:dC	9.2 ± 1.4	6.8 ± 1.8	1.4 ± 0.4	160 ± 20	74 ± 4	2.2 ± 0.3
OdI:dA	81 ± 6	7.6 ± 1.5	11 ± 2	900 ± 180	32 ± 9	28 ± 10
SdI:dC	0.23 ± 0.04	5.6 ± 0.3	0.041 ± 0.007	10 ± 4	61 ± 20	0.16 ± 0.08
SdI:dA	94 ± 25	8.4 ± 2.4	11 ± 4	650 ± 200	42 ± 8	16 ± 6

[a]Averages ± standard deviations calculated from three or more experiments.

Combining the data from dCTP and dATP insertion, we found that with KF-exo, CdG preferentially directs dATP insertion, while OdG, and SdG to an even larger extent, both preferentially direct dCTP incorporation. With BF, CdG preferentially directs dCTP insertion, while OdG and SdG preferentially direct dATP insertion. With both enzymes, OdI and SdI preferentially direct dATP insertion, with the preference switched relative to that of OdG and SdG with KF-exo.

Extension past XdG:dC and XdG:dA Base Pairs. Single-nucleotide extensions with KF-exo and BF were also studied for those pairs tested during the incorporation experiments [except past the dI:dA base pair because of the low activity of that reaction (see Figures S3 and S4 of the Supporting Information)]. Steady state kinetics were again used, but the 15-nucleotide templates were now paired with radiolabeled 11-nucleotide primers that contained either a dC or dA opposite dG, OdG, or one of the analogues (Table 3). In accordance with previous results with KF-exo,[21,30] extension past an OdG:dA base pair was more efficient than past an OdG:dC base pair. Turing to the work with the new analogues, we found the relative extension efficiencies past XdG:dC pairs were similar for both enzymes and somewhat mirrored the incorporation of dCTP (Table 2). All efficiencies were reduced compared to that of extension past dG:dC base pairs (though much less so for BF), but efficiencies of extension past OdG:dC and SdG:dC base pairs were reduced even as compared to efficiencies of extension past CldG:dC and BrdG:dC base pairs. Upon comparison of the dCTP insertion and extension results between enzymes, BF appears more sensitive than KF-exo to alterations in the imidazole ring of dG/OdG during dCTP incorporation, but less sensitive than KF-exo during extension past the resulting base pairs. Results from extensions past XdG:dA base pairs did not mirror the incorporation of dATP for either enzyme but were similar to each other; extensions past OdG:dA and SdG:dA base pairs were not only relatively equal but also more efficient than those past CdG:dA base pairs. BF was also more accommodating of XdG:dA base pairs at the postinsertion site than KF-exo, with extension past OdG:dA base pairs being almost as efficient as that past dG:dC base pairs. With both enzymes, extensions past OdI:dA and SdI:dA base pairs were slightly less efficient (3−5-fold) than past OdG:dA and SdG:dA base pairs, respectively.

DISCUSSION

Incorporation of dCTP opposite dG, OdG, and Their Analogues. Previous work with purine monomers supports the theory that the presence of a large atom off C8 induces a preference for a syn conformation about the glycosidic bond.[46,53] It has been suggested that this preference is due to a destabilized anti conformation attributable to a clash between the large C8 atom and the nucleoside sugar.[23,24] This same destabilizing interaction is also thought to be responsible, at least in part, for the decreased stability of OdG:dC base pairs where the anti conformation is used; consistent with this theory, duplexes that contain a CldG:dC, BrdG:dC, or 8-methyldG:dC base pair all show decreased melting temperatures relative to that of a similar duplex containing a dG:dC base pair (Table 1).[46,56] Additionally, even within the series CdG, OdG, and SdG, which all contain a hydrogen at N7, base pairs to dC become more unstable as the atomic size off C8 increases.[47]

dCTP incorporation with KF-exo and BF mirrors, to some degree, the melting data summarized above. The dCTP binding affinities and overall efficiencies of incorporation opposite CldG and BrdG, and OdG and SdG, were all reduced compared to those for incorporation opposite dG and CdG, respectively (Figure 1). Thus, the same negative interaction with a large C8 atom that leads to the reduced stability of these base pairs may also help reduce the efficiency of incorporation of dCTP opposite the individual nucleotides. These new findings are also in accordance with much previous work that suggests the high fidelity displayed by A family polymerases stems from them having "tight" insertion sites that are sensitive to steric changes.[57−60] While the standard Watson−Crick (W−C) base pairs, dG:dC, dC:dG, dA:dT, and dT:dA, all have similar shapes and H8(purine)−H5(pyrimidine) distances, the overall base pair shape and H8−H5 distance would be significantly increased if dCTP is incorporated opposite CldG, BrdG, OdG, SdG, OdI, or SdI. Thus, if the polymerase insertion site is

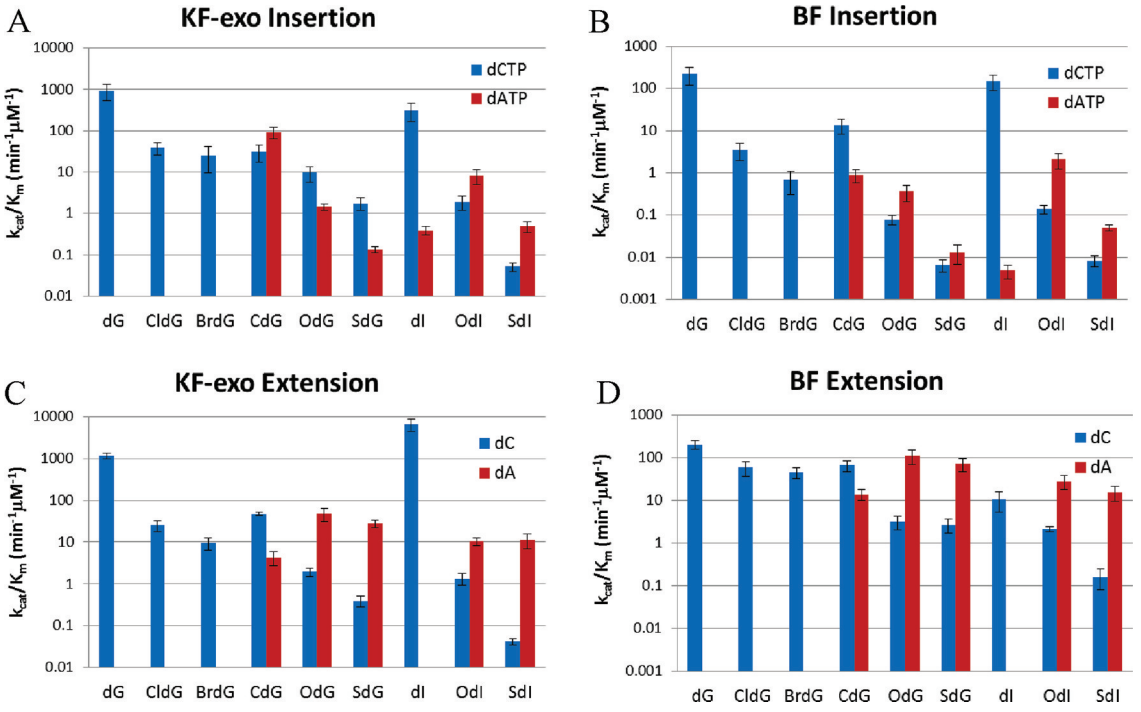

Figure 1. Graphical representations of the KF-exo (A) and BF (B) incorporation efficiencies listed in Table 2 and the KF-exo (C) and BF (D) extension efficiencies listed in Table 3. Note the *y*-axes are on a logarithmic scale.

normally rigid and tightly defined around the cognate W−C base pair shape, detrimental clashing interactions could develop as larger atoms are substituted at the C8 position of dG or OdG.

Crystallographic studies published with BF, where the enzyme was cocrystallized with a template dG paired to dCTP in the insertion site, may also provide some insight into these results.[42] The structure (Protein Data Bank entry 1LV5) shows Ile716 and the sugar ring of OdG are both in the proximity (within 3.5 Å) of C8 of dG and could lead to clashing interactions, and possible distortions at the insertion site, should a large atom be substituted off C8 (see Figures S4 and S5 of the Supporting Information). Distortions in the DNA and protein have already been observed in a ternary structure of BF that contained an OdG:dC base pair in the postinsertion site.[34] The presence of analogous perturbations in the insertion site (due to potential clashing with Ile716) of BF could help to explain the significant decreases in dCTP incorporation efficiency observed opposite the analogues with large atoms off C8.

Though KF-exo and BF show similar trends with respect to dCTP incorporation, BF appears to be more sensitive to structural perturbations within the imidazole ring of dG or OdG. As compared to that opposite dG, the efficiency of insertion of dCTP opposite BrdG was decreased 36-fold with KF-exo but 310-fold with BF, while the efficiency of insertion opposite SdG was decreased 510-fold with KF-exo and 34000-fold with BF. This difference in reactivity may be explained, in part, by subtle differences in the active site between KF-exo and BF. For example, the amino acid analogous to Ile716 (in BF) is Met768 in KF-exo. The different shapes of these two amino acids, as well as the known flexibility of methionine side chains,[61,62] may help lead to the slightly different sensitivities to atomic size off C8 observed between KF-exo and BF.

However, the size of the C8 atom may not be the only influencing factor during single-nucleotide insertion. Despite containing similarly sized or smaller atoms off C8, dCTP was incorporated less efficiently opposite OdG and SdG as compared to CldG and BrdG with both KF-exo and BF. It has been well established that the 8-keto tautomer of OdG predominates at neutral pH,[18,19] and on the basis of studies with 8-thio-G,[63] and 8-thio-A,[53] and 6-thioguanine, 6-thio-G, and 6-thio-dG,[64−66] the corresponding 8-keto tautomer of SdG is expected to predominate, as well. Thus, the electronics of the imidazole ring of OdG and SdG are expected to be opposite that of dG (see Figure S9 of the Supporting Information) and may lead to additional unfavorable interactions with the polymerase or the nucleotide sugar. The reduction in dCTP incorporation efficiency opposite the C nucleotide CdG relative to dG with both enzymes is also consistent with other factors besides sterics playing a role during dCTP incorporation; it is possible this reduction is due to the opposite electrostatic potential at N7 between dG and CdG (similar to OdG and SdG) and/or the C nucleotide character of CdG that causes structural changes as compared to the N nucleotides.[47] Nonetheless, upon examination of the OdG analogues in which a N7-hydrogen is present (CdG, OdG, SdG, OdI, and SdI), there is still a significant decrease in dCTP incorporation efficiency with both KF-exo and BF as the size of the atom off C8 increases. Thus, while factors like electronics may also be significant, it is still likely that steric clashing at C8 hinders, at least to some extent, the incorporation of dCTP opposite OdG, increasing the mutagenic potential of OdG with both enzymes.

Incorporation of dATP opposite OdG and Its Analogues. CdG:dA base pairs are less stable than either OdG:dA/SdG:dA or OdI:dA/SdI:dA base pairs, while the stabilities within each set are similar (Table 1).[47] However, dATP insertions with KF-exo and BF were most efficient opposite CdG and least efficient opposite SdG and SdI (Figure 1).

dx.doi.org/10.1021/bi201383c | *Biochemistry* 2011, 50, 10713−10723

Thus, the observed differences in incorporation activity cannot be explained by the inherent base pair stabilities, and similar to dCTP incorporation, it appears the presence of a large atom off C8 in the template (now in the minor groove) also leads to a decreased dATP incorporation efficiency.

Previously published crystallographic and biochemical data for other replicative polymerases have indicated a specific minor groove tyrosine may help to keep the insertion site rigid and hostile to steric perturbations.[25,67] The analogous amino acids in KF-exo and BF are Tyr766 and Tyr714, respectively, and mutation of Tyr766 has been shown to substantially decrease the replication fidelity with KF-exo.[68] Thus, these two residues may play a similar role in keeping the insertion site of KF-exo and BF tightly formed and inflexible, disallowing mismatches that vary in size from the standard W−C base pairs in the minor groove (see Figures S5 and S7 of the Supporting Information). Consistent with this theory, a disease-associated mutation of the corresponding tyrosine (Y955C) in another A family polymerase, human mitochondrial polymerase γ, also yielded a significantly decreased preference for incorporation of dCTP over dATP opposite OdG.[69] Via application of this information to the results presented in Figure 1, it is possible CdG, which lacks a large atom off C8, has fewer destabilizing interactions present when directing dATP incorporation, thus allowing the reaction to be relatively efficient. Conversely, the lower efficiencies of incorporation of dATP opposite SdG and SdI relative to that opposite CdG, OdG, and OdI may be due to minor groove clashing (possibly with the minor groove Tyr) caused by the larger atomic size and longer bond length of sulfur, as well as the possible opening of the base pair that is known to occur with modified nucleotides that contain a thio group at or near the hydrogen bonding face.[64−66,70]

Expanding on this idea, we theorized that the C2-exocyclic amine would also create clashing interactions in the major groove of the insertion site because it would also lie outside the cognate W−C base pair shape, similar to when a large atom is present off C8 of dG during dCTP incorporation (see Figure S6 of the Supporting Information). Biochemical results reported herein, and previously with KF-exo,[39] are consistent with this theory; removal of the C2-exocyclic amine (to form OdI and SdI) leads to an increased dATP incorporation activity, as well as an overall preference for dATP insertion. Additionally, previous work has shown a nonpolar isostere of OdI containing a chlorine at C8 also preferentially directs dATP incorporation with KF-exo.[41] Thus, it appears that the presence of the C2-exocyclic amine and a large atom at C8 may each reduce the efficiency of incorporation of dATP opposite OdG and its analogues.

Extension past Base Pairs Containing dG, OdG, and Their Analogues. Previous studies have shown that KF-exo extends past OdG:dC base pairs less efficiently than past dG:dC base pairs (at the T1:P1 site).[30] This is also true for BF, which extended past OdG:dC base pairs with a 63-fold lower efficiency than past dG:dC base pairs (Table 2). Additionally, efficiencies of extension past all of the XdG:dC/XdI:dC base pairs were reduced relative to efficiencies of extension past dG:dC/dI:dC base pairs (though less so for BF), similar to the results gathered during dCTP incorporation. Thus, it appears that the presence of a large atom off C8 of a template dG/OdG can lead not only to reduced dCTP insertion activity but also to reduced extension efficiency as the resulting pair moves out of the insertion site. The crystallographic data for BF mentioned previously are consistent with this finding and show significant backbone perturbation in the postinsertion site when an OdG:dC base pair is present.[34] Interestingly, similar backbone distortions are also seen when DNA mismatches occupy the BF postinsertion site;[43] thus, it appears that these polymerases may view OdG:dC and XdG:dC/XdI:dC base pairs like DNA mismatches and select against their extension. Finally, similar to the incorporation experiments with both polymerases, efficiencies of extension past OdG:dC and SdG:dC base pairs were reduced even as compared to efficiencies of extension past CldG:dC and BrdG:dC base pairs. Thus, as with single-nucleotide incorporation, factors other than atomic size off C8 at the T1 site, like electronics, may also play a role during single-nucleotide extension with these polymerases.

It is worth noting that with KF-exo, extension past a dI:dC base pair was more efficient than past a dG:dC base pair, even though the opposite was true for BF, and extensions past OdI:dC and SdI:dC base pairs were less efficient than past OdG:dC and SdG:dC base pairs with both enzymes. When paired to dG, the C2-oxygen of dC (at the P1 site) is known to make a hydrogen bond not only to the C2-exocyclic amine of dG but also to Arg668 of KF-exo (Arg615 of BF).[71−73] It is possible that the loss of the C2-exocyclic amine allows for a more optimal interaction between the C2-oxygen and Arg668 only with KF-exo and only when dI, and not OdI or SdI, is at the T1 site; however, this hypothesis is speculative at this point.

As for extensions past XdG:dA base pairs, the results reported herein are consistent with previously published work with KF-exo.[30] Extension past an OdG:dA base pair was more efficient than past an OdG:dC base pair with both polymerases. The reasons for the relatively high extension activity past OdG:dA base pairs can be explained, at least in part, by a published ternary structure of BF with an OdG:dA base pair in the postinsertion site.[34] The structure indicates there are few structural perturbations during extension past OdG:dA base pairs (unlike past OdG:dC base pairs), and the C8-oxygen of the OdG:dA base pair (and presumably the C8-sulfur of the SdG:dA base pair) is able to preserve a minor groove hydrogen bond to Gln797. CdG does not have the ability to accept hydrogen bonds at C8 and cannot interact with Gln797, thus explaining the decreased efficiency of extension past CdG:dA base pairs relative to OdG:dA and SdG:dA base pairs. KF-exo has an analogous glutamine (Gln849), and it is possible a similar interaction is involved with this polymerase, however, previous biochemical studies may not classify it as essential because much larger reductions in efficiency have been observed when other minor groove hydrogen bonds are eliminated, for example, the interaction between Arg668 of KF-exo and the minor groove face of P1 discussed above. Finally, opposite to what was observed during incorporation of dATP, removal of the C2-exocyclic amine (to form OdI:dA and SdI:dA base pairs) led to 3−5-fold less efficient extension reactions with both enzymes. The reasons for this observation are unclear, though it is possible a stabilizing interaction could exist between the C2-exocyclic amine and the DNA phosphate backbone; this theory has been proposed previously with other DNA polymerases[25,74] and appears to be plausible on the basis of crystallographic studies with BF (see Figure S8 of the Supporting Information).

■ CONCLUSION

Though KF-exo and BF have contrary dCTP versus dATP incorporation preferences opposite OdG, with the analogues studied herein they behave quite similarly overall. They show

analogous trends not only in dCTP and dATP incorporation activity as the size and/or electronics within the imidazole ring of a template dG or OdG are altered but also in dATP incorporation efficiency as the C2-exocyclic amine is removed from OdG and SdG; the two enzymes also roughly mirror each other with respect to extension. The reason for their contrary incorporation preferences opposite OdG is subtle and appears to be due to BF being more sensitive to alterations in the imidazole ring of dG during dCTP incorporation. In other words, while with each enzyme the efficiencies of incorporation of both dCTP and dATP opposite OdG are reduced as compared to the efficiency of dCTP incorporation opposite dG, it is the differing extents of these reductions that determine the incorporation preference and, thus, the mutagenic potential of OdG. This holds true for the incorporation preferences opposite CdG, SdG, OdI, and SdI, as well.

We did wonder if stacking and/or solvation effects in the template could play a role during incorporation; however, no clear correlation emerged between activity and either electrostatic potential or stacking ability alone, as judged by surface area and polarizability (see Table S1 and Figure S9 of the Supporting Information).

More studies with these analogues are needed in the future. It will be useful to study their activities with the polymerases using pre-steady state (single-turnover) kinetic experiments in which the individual steps of nucleotide insertion can be analyzed.[30] It will also be important to expand these studies to additional polymerases, including those in the B family like RB69,[25,26] X family like pol β,[74] and Y family like Dpo4[28] and polκ,[32] as well as the less closely related A family DNA polymerase from bacteriophage T7.[29,67] These polymerases are believed to have various mechanisms for triphosphate selectivity opposite OdG, and ternary crystal structures with an OdG in the insertion site are available in each case. Comparisons between the published structures and biochemical experiments with our analogues will likely provide additional insights into the factors that influence OdG-initiated mutation and, thus, the link between OdG and aging and disease.

■ ASSOCIATED CONTENT

Supporting Information

Qualitative incorporation experiments with all natural dNTPs; qualitative extension past dG, OdG, and their analogues when paired with dC or dA; interpretations of previously published BF crystal structure data; calculations of physical properties; characterization of synthesized oligonucleotides; ^{1}H and ^{13}C NMR spectra of compounds **2** and **3**; and ^{31}P NMR spectra of compound **4**. This material is available free of charge via the Internet at http://pubs.acs.org.

■ AUTHOR INFORMATION

Corresponding Author

*E-mail: mhamm@richmond.edu. Telephone: (804) 287-6327. Fax: (804) 287-1897.

Funding

This work was supported by the University of Richmond and the NSF-CAREER (CHE-0239664) and NSF-RUI (CHE-0956474) programs. M.L.H. is a Henry Dreyfus Teacher-Scholar.

■ ACKNOWLEDGMENTS

We thank Marc Greenberg for the generous gift of OdI phosphoramidite, Bojan Dragulev for help with DNA synthesis, and Eugene Wu for help with PyMOL and Coot and for critical reading of the manuscript.

■ REFERENCES

(1) Kasai, H., and Nishimura, S. (1991) Formation of 8-Hydroxydeoxyguanosine in DNA by Oxygen Radicals and its Biological Significance. In *Oxidative Stress: Oxidants and Antioxidants* (Sies, H., Ed.) pp 99−116, Academic Press, San Diego.

(2) Cadet, J., Douki, T., Gasparutto, D., and Ravanat, J. L. (2003) Oxidative damage to DNA: Formation, measurement and biochemical features. *Mutat. Res. 531*, 5−23.

(3) Vallyathan, V., Shi, X. L., and Castranova, V. (1998) Reactive oxygen species: Their relation to pneumoconiosis and carcinogenesis. *Environ. Health Perspect. 106*, 1151−1155.

(4) Dizdaroglu, M. (1985) Formation of 8-hydroxyguanine moiety in deoxyribonucleic acid on γ-irradiation in aqueous solution. *Biochemistry 24*, 4476−4481.

(5) Floyd, R. (1990) The role of 8-hydroxyguanine in carcinogenesis. *Carcinogenesis 11*, 1447−1450.

(6) Hutchinson, F. (1985) Chemical Changes Induced in DNA by Ionizing Radiation. *Prog. Nucleic Acid Res. Mol. Biol. 32*, 115−154.

(7) Pryor, W. A. (1986) Oxy-radicals and related species: Their formation, lifetimes, and reactions. *Annu. Rev. Physiol. 48*, 657−667.

(8) Ames, B., Shigenaga, M., and Hagen, T. (1993) Oxidants, antioxidants, and the degenerative diseases of aging. *Proc. Natl. Acad. Sci. U.S.A. 90*, 7915−7922.

(9) Cheng, K. C., Cahill, D. S., Kasai, H., Nishimura, S., and Loeb, L. A. (1992) 8-Hydroxyguanine, an Abundant Form of Oxidative DNA Damage, Causes G → T and A → C Substitutions. *J. Biol. Chem. 267*, 166−172.

(10) Le Page, F., Margot, A., Grollman, A. P., Sarasin, A., and Gentil, A. (1995) Mutagenicity of a unique 8-oxoguanine in a human Ha-ras sequence in mammalian cells. *Carcinogenesis 16*, 2779−2784.

(11) Hamilton, M., Van Remmen, H., Drake, J., Yang, H., Guo, Z., Kewitt, K., Walter, C., and Richardson, A. (2001) Does oxidative damage to DNA increase with age? *Proc. Natl. Acad. Sci. U.S.A. 98*, 10469−10474.

(12) Muscari, C., Giaccari, A., Giordano, E., Clo, C., Guarnieri, C., and Caldarera, C. (1996) Role of reactive oxygen species in cardiovascular aging. *Mol. Cell. Biochem. 160−161*, 159−166.

(13) Orr, W. C., and Sohal, R. S. (1994) Extension of Life-Span by Overexpression of Superoxide-Dismutase and Catalase in *Drosophila melanogaster*. *Science 263*, 1128−1130.

(14) Bashir, S., Harris, G., Denman, M., Blake, D., and Winyard, P. (1993) Oxidative DNA damage and cellular sensitivity to oxidative stress in human autoimmune diseases. *Ann. Rheum. Dis. 52*, 659−666.

(15) Marnett, L. J. (2000) Oxyradicals and DNA damage. *Carcinogenesis 21*, 361−370.

(16) Dziaman, T., Huzarski, T., Gackowski, D., Rozalski, R., Siomek, A., Szpila, A., Guz, J., Lubinski, J., and Olinski, R. (2009) Elevated level of 8-oxo-7,8-dihydro-2′-deoxyguanosine in leukocytes of BRCA1 mutation carriers compared to healthy controls. *Int. J. Cancer 125*, 2209−2213.

(17) Evans, M. D., Dizdaroglu, M., and Cooke, M. S. (2004) Oxidative DNA damage and disease: Induction, repair and significance. *Mutat. Res. 567*, 1−61.

(18) Culp, S. J., Cho, B. P., Kadlubar, F. F., and Evans, F. E. (1989) Structural and conformational analyses of 8-hydroxy-2′-deoxyguanosine. *Chem. Res. Toxicol. 2*, 416−422.

(19) Jang, Y. H., Goddard, W. A., Noyes, K. T., Sowers, L. C., Hwang, S., and Chung, D. S. (2002) First Principles Calculations of the Tautomers and pKa Values of 8-Oxoguanine: Implications for Mutagenicity and Repair. *Chem. Res. Toxicol. 15*, 1023−1035.

(20) Plum, G., Grollman, A., Johnson, F., and Breslauer, K. (1995) Influence of the Oxidatively Damaged Adduct 8-Oxodeoxyguanosine

on the Conformation, Energetics, and Thermodynamic Stability of a DNA Duplex. *Biochemistry 34*, 16148−16160.
(21) Kouchakdjian, M., Bodepudi, V., Shibutani, S., Eisenberg, M., Johnson, F., Grollman, A., and Patel, D. (1991) NMR structural studies of the ionizing radiation adduct 7-hydro-8-oxodeoxyguanosine (8-oxo-7H-dG) opposite deoxyadenosine in a DNA duplex. 8-Oxo-7H-dG(syn)·dA(anti) alignment at lesion site. *Biochemistry 30*, 1403−1412.
(22) McAuley-Hecht, K., Leonard, G., Gibson, N., Thomson, J., Watson, W., Hunter, W., and Brown, T. (1994) Crystal structure of a DNA duplex containing 8-hydroxydeoxyguanine-adenine base pairs. *Biochemistry 33*, 10266−10270.
(23) Lipscomb, L., Peek, M., Morningstar, M., Verghis, S., Miller, E., Rich, A., Essigmann, J., and Williams, L. (1995) X-ray structure of a DNA decamer containing 7,8-dihydro-8-oxoguanine. *Proc. Natl. Acad. Sci. U.S.A. 92*, 719−723.
(24) Oda, Y., Uesugi, S., Ikehara, M., Nishimura, S., Kawase, Y., Ishikawa, H., Inoue, H., and Ohtsuka, E. (1991) NMR studies of a DNA containing 8-hydroxydeoxyguanosine. *Nucleic Acids Res. 19*, 1407−1412.
(25) Beckman, J., Wang, M. N., Blaha, G., Wang, J. M., and Konigsberg, W. H. (2010) Substitution of Ala for Tyr567 in RB69 DNA Polymerase Allows dAMP To Be Inserted opposite 7,8-Dihydroxy-8-oxoguanine. *Biochemistry 49*, 4116−4125.
(26) Freisinger, E., Grollman, A. P., Miller, H., and Kisker, C. (2004) Lesion (in)tolerance reveals insights into DNA replication fidelity. *EMBO J. 23*, 1494−1505.
(27) Eoff, R. L., Irimia, A., Angel, K. C., Egli, M., and Guengerich, P. (2007) Hydrogen bonding of 7,8-dihydro-8-oxodeoxyguanosine with a charged residue in the little finger domain determines miscoding events in *Sulfolobus solfataricus* DNA polymerase Dpo4. *J. Biol. Chem. 282*, 19831−19843.
(28) Zang, H., Irimia, A., Choi, J. Y., Angel, K. C., Loukachevitch, L. V., Egli, M., and Guengerich, F. P. (2006) Efficient and high fidelity incorporation of dCTP opposite 7,8-dihydro-8-oxodeoxyguanosine by *Sulfolobus solfataricus* DNA polymerase Dpo4. *J. Biol. Chem. 281*, 2358−2372.
(29) Furge, L. L., and Guengerich, F. P. (1997) Analysis of nucleotide insertion and extension at 8-oxo-7,8-dihydroguanine by replicative T7 polymerase exo(−) and human immunodeficiency virus-1 reverse transcriptase using steady-state and pre-steady-state kinetics. *Biochemistry 36*, 6475−6487.
(30) Lowe, L. G., and Guengerich, F. P. (1996) Steady-state and pre-steady-state kinetic analysis of dNTP insertion opposite 8-oxo-7,8-dihydroguanine by *Escherichia coli* polymerases I exo(−) and II exo(−). *Biochemistry 35*, 9840−9849.
(31) Miller, H., Prasad, R., Wilson, S. H., Johnson, F., and Grollman, A. P. (2000) 8-OxodGTP incorporation by DNA polymerase β is modified by active-site residue Asn279. *Biochemistry 39*, 1029−1033.
(32) Irimia, A., Eoff, R. L., Guengerich, F. P., and Egli, M. (2009) Structural and Functional Elucidation of the Mechanism Promoting Error-prone Synthesis by Human DNA Polymerase κ Opposite the 7,8-Dihydro-8-oxo-2′-deoxyguanosine Adduct. *J. Biol. Chem. 284*, 22467−22480.
(33) Maga, G., Villani, G., Crespan, E., Wimmer, U., Ferrari, E., Bertocci, B., and Hubscher, U. (2007) 8-Oxo-guanine bypass by human DNA polymerases in the presence of auxiliary proteins. *Nature 447*, 606−608.
(34) Hsu, G. W., Ober, M., Carell, T., and Beese, L. S. (2004) Error-prone replication of oxidatively damaged DNA by a high-fidelity DNA polymerase. *Nature 431*, 217−221.
(35) Kiefer, J. R., Mao, C., Hansen, C. J., Basehore, S. L., Hogrefe, H. H., Braman, J. C., and Beese, L. S. (1997) Crystal structure of a thermostable *Bacillus* DNA polymerase I large fragment at 2.1 angstrom resolution. *Structure 5*, 95−108.
(36) Kiefer, J. R., Mao, C., Braman, J. C., and Beese, L. S. (1998) Visualizing DNA replication in a catalytically active *Bacillus* DNA polymerase crystal. *Nature 391*, 304−307.
(37) Chen, L. S., Bahr, M. H., and Sheppard, T. L. (2003) Effects of 8-chlorodeoxyadenosine on DNA synthesis by the Klenow fragment of DNA polymerase I. *Bioorg. Med. Chem. Lett. 13*, 1509−1512.
(38) Einolf, H. J., Schnetz-Boutaud, N., and Guengerich, F. P. (1998) Steady-state and pre-steady-state kinetic analysis of 8-oxo-7,8-dihydroguanosine triphosphate incorporation and extension by replicative and repair DNA polymerases. *Biochemistry 37*, 13300−13312.
(39) Oka, N., and Greenberg, M. M. (2005) The effect of the 2-amino group of 7,8-dihydro-8-oxo-2′-deoxyguanosine on translesion synthesis and duplex stability. *Nucleic Acids Res. 33*, 1637−1643.
(40) Sintim, H. O., and Kool, E. T. (2006) Enhanced base pairing and replication efficiency of thiothymidines, expanded-size variants of thymidine. *J. Am. Chem. Soc. 128*, 396−397.
(41) Taniguchi, Y., and Kool, E. T. (2007) Nonpolar isosteres of damaged DNA bases: Effective mimicry of mutagenic properties of 8-oxopurines. *J. Am. Chem. Soc. 129*, 8836−8844.
(42) Johnson, S. J., Taylor, J. S., and Beese, L. S. (2003) Processive DNA synthesis observed in a polymerase crystal suggests a mechanism for the prevention of frameshift mutations. *Proc. Natl. Acad. Sci. U.S.A. 100*, 3895−3900.
(43) Johnson, S. J., and Beese, L. S. (2004) Structures of mismatch replication errors observed in a DNA polymerase. *Cell 116*, 803−816.
(44) Russo, M., Jimenez, L. B., Mulazzani, Q. G., D'Angelantonio, M., Guerra, M., Miranda, M. A., and Chatgilialoglu, C. (2006) Chemical radiation studies of 8-bromo-2′-deoxyinosine and 8-bromoinosine in aqueous solutions. *Chem.—Eur. J. 12*, 7684−7693.
(45) Hamm, M., Cholera, R., Hoey, C., and Gill, T. (2004) Oligonucleotide incorporation of 8-thio-2′-deoxyguanosine. *Org. Lett. 6*, 3817−3820.
(46) Hamm, M. L., Rajguru, S., Downs, A. M., and Cholera, R. (2005) Base pair stability of 8-chloro- and 8-iodo-2′-deoxyguanosine opposite 2′-deoxycytidine: Implications regarding the bioactivity of 8-oxo-2′-deoxyguanosine. *J. Am. Chem. Soc. 127*, 12220−12221.
(47) Hamm, M. L., Parker, A. J., Steele, T. W. E., Carman, J. L., and Parish, C. A. (2010) Oligonucleotide Incorporation and Base Pair Stability of 9-Deaza-2′-deoxyguanosine, an Analogue of 8-Oxo-2′-deoxyguanosine. *J. Org. Chem. 75*, 5661−5669.
(48) Eason, R. G., Burkhardt, D. M., Phillips, S. J., Smith, D. P., and David, S. S. (1996) Synthesis and characterization of 8-methoxy-2′-deoxyadenosine-containing oligonucleotides to probe the syn glycosidic conformation of 2′-deoxyadenosine within DNA. *Nucleic Acids Res. 24*, 890−897.
(49) Martin, F. H., Castro, M. M., Aboulela, F., and Tinoco, I. (1985) Base-Pairing Involving Deoxyinosine: Implications for Probe Design. *Nucleic Acids Res. 13*, 8927−8938.
(50) Singh, S. K., Szulik, M. W., Ganguly, M., Khutsishvili, I., Stone, M. P., Marky, L. A., and Gold, B. (2011) Characterization of DNA with an 8-oxoguanine modification. *Nucleic Acids Res. 39*, 6789−6801.
(51) Uesugi, S., Oda, Y., Ikehara, M., Kawase, Y., and Ohtsuka, E. (1987) Identification of I-A Mismatch Base-Pairing Structure in DNA. *J. Biol. Chem. 262*, 6965−6968.
(52) Corfield, P. W. R., Hunter, W. N., Brown, T., Robinson, P., and Kennard, O. (1987) Inosine.Adenine Base-Pairs in a B-DNA Duplex. *Nucleic Acids Res. 15*, 7935−7949.
(53) Uesugi, S., and Ikehara, M. (1977) Carbon-13 magnetic resonance spectra of 8-substituted purine nucleosides. Characteristic shifts for the syn conformation. *J. Am. Chem. Soc. 99*, 3250−3253.
(54) Cysewski, P. (1998) An ab initio study of the tautomeric and coding properties of 8-oxo-guanine. *J. Chem. Soc., Faraday Trans. 94*, 3117−3125.
(55) Venkateswarlu, D., and Leszczynski, J. (1998) Tautomeric equilibria in 8-oxopurines: Implications for mutagenicity. *J. Comput.-Aided Mol. Des. 12*, 373−382.
(56) Kohda, K., Tsunomoto, H., Minoura, Y., Tanabe, K., and Shibutani, S. (1996) Synthesis, Miscoding Specificity, and Thermodynamic Stability of Oligodeoxynucleotide Containing 8-Methyl-2′-deoxyguanosine. *Chem. Res. Toxicol. 9*, 1278−1284.

(57) Kim, T. W., Delaney, J. C., Essigmann, J. M., and Kool, E. T. (2005) Probing the active site tightness of DNA polymerase in subangstrom increments. *Proc. Natl. Acad. Sci. U.S.A. 102*, 15803−15808.
(58) Kool, E. T. (2002) Active site tightness and substrate fit in DNA replication. *Annu. Rev. Biochem. 71*, 191−219.
(59) Sintim, H. O., and Kool, E. T. (2006) Remarkable sensitivity to DNA base shape in the DNA polymerase active site. *Angew. Chem., Int. Ed. 45*, 1974−1979.
(60) Streckenbach, F., Rangam, G., Moller, H. M., and Marx, A. (2009) Steric Constraints Dependent on Nucleobase Pair Orientation Vary in Different DNA Polymerase Active Sites. *ChemBioChem 10*, 1630−1633.
(61) Siivari, K., Zhang, M. J., Palmer, A. G., and Vogel, H. J. (1995) NMR Studies of the Methionine Methyl-Groups in Calmodulin. *FEBS Lett. 366*, 104−108.
(62) Gellman, S. H. (1991) On the Role of Methionine Residues in the Sequence-Independent Recognition of Nonpolar Protein Surfaces. *Biochemistry 30*, 6633−6636.
(63) Cho, B., Kadlubar, F., Culp, S., and Evans, F. (1990) Nitrogen-15 nuclear magnetic resonance studies on the tautomerism of 8-hydroxy-2′-deoxyguanosine, 8-hydroxyguanosine, and other C8-substituted guanine nucleosides. *Chem. Res. Toxicol. 3*, 445−452.
(64) Bugg, C. E., and Thewalt, U. L. F. (1970) Crystal and Molecular Structure of 6-Thioguanine. *J. Am. Chem. Soc. 92*, 7441−7445.
(65) Somerville, L., Krynetski, E. Y., Krynetskaia, N. F., Beger, R. D., Zhang, W. X., Marhefka, C. A., Evans, W. E., and Kriwacki, R. W. (2003) Structure and dynamics of thioguanine-modified duplex DNA. *J. Biol. Chem. 278*, 1005−1011.
(66) Thewalt, U., and Bugg, C. E. (1972) Effects of Sulfur Substituents on Base Stacking and Hydrogen Bonding. The Crystal Structure of 6-Thioguanosine Monohydrate. *J. Am. Chem. Soc. 94*, 8892−8898.
(67) Brieba, L. G., Eichman, B. F., Kokoska, R. J., Doublie, S., Kunkel, T. A., and Ellenberger, T. (2004) Structural basis for the dual coding potential of 8-oxoguanosine by a high-fidelity DNA polymerase. *EMBO J. 23*, 3452−3461.
(68) Carroll, S. S., Cowart, M., and Benkovic, S. J. (1991) A Mutant of DNA-Polymerase-I (Klenow Fragment) with Reduced Fidelity. *Biochemistry 30*, 804−813.
(69) Graziewicz, M. A., Bienstock, R. J., and Copeland, W. C. (2007) The DNA polymerase γ Y955C disease variant associated with PEO and parkinsonism mediates the incorporation and translesion synthesis opposite 7,8-dihydro-8-oxo-2′-deoxyguanosine. *Hum. Mol. Genet. 16*, 2729−2739.
(70) Diop-Frimpong, B., Prakash, T. P., Rajeev, K. G., Manoharan, M., and Egli, M. (2005) Stabilizing contributions of sulfur-modified nucleotides: Crystal structure of a DNA duplex with 2′-O-[2-(methoxy)ethyl]-2-thiothymidines. *Nucleic Acids Res. 33*, 5297−5307.
(71) Morales, J. C., and Kool, E. T. (2000) Functional hydrogen-bonding map of the minor groove binding tracks of six DNA polymerases. *Biochemistry 39*, 12979−12988.
(72) Spratt, T. E. (2001) Identification of hydrogen bonds between *Escherichia coli* DNA polymerase I (Klenow fragment) and the minor groove of DNA by amino acid substitution of the polymerase and atomic substitution of the DNA. *Biochemistry 40*, 2647−2652.
(73) Meyer, A. S., Blandino, M., and Spratt, T. E. (2004) *Escherichia coli* DNA polymerase I (Klenow fragment) uses a hydrogen-bonding fork from Arg(668) to the primer terminus and incoming deoxynucleotide triphosphate to catalyze DNA replication. *J. Biol. Chem. 279*, 33043−33046.
(74) Krahn, J. M., Beard, W. A., Miller, H., Grollman, A. P., and Wilson, S. H. (2003) Structure of DNA polymerase β with the mutagenic DNA lesion 8-oxodeoxyguanine reveals structural insights into its coding potential. *Structure 11*, 121−127.